

Article

Precision maize stand analysis using remote sensing methods: plant density measurement with spectral data integration

Árpád Illés, Éva Horváth, Péter Zagyi*, Csaba Bojtor, Adrienn Széles

Institute of Land Use, Engineering and Precision Farming Technology, Faculty of Agricultural and Food Sciences and Environmental Management, University of Debrecen, Böszörményi út 138, H-4032 Debrecen, Hungary; horvath.eva@agr.unideb.hu (É.H.); illes.arpad@agr.unideb.hu (Á.I.); bojtor.csaba@agr.unideb.hu (C.B.); szelesa@agr.unideb.hu (A.S.)

* Correspondence: zagyi.peter@agr.unideb.hu

Abstract: The aim of this study was to use remote sensing with a drone equipped with a multispectral camera to take a stand survey of maize after the phenological stage of emergence, and to count the number of emerged plants and determine its accuracy. Our investigations were carried out at the University of Debrecen, Látókép Production Experimental Station in a sowing date long-term experiment. In the 2024 growing season, Sowing Date I was on 4 April and Sowing Date II on 12 April. The same maize hybrids with 8-8 different genotypes were used for each sowing date. There is a strong correlation between number of plants/plot and number of plants/rowx2 for the two plant density measurements presented in this paper, with an r value of 0.977*** ($p < 0.001$). Among the plant density and NDVI values, the correlation between number of plants/rowx2 at the second measurement time (July 4) was significant at $r = -0.418$ ***. The analysis of the relationship between number of rows and yield showed that the hybrids included in the study compensated well for differences in number of rows due to sowing or emergence and this did not translate into an increase or decrease in yield. By using the plant density count method and results to identify emergence imbalances, farmers can correct their crop stand management strategies in a timely manner. Knowing the exact number of plants can also be important for subsequent agrotechnical decisions.

Keywords: maize, plant population, remote sensing, seeding, sowing date, vegetation index

Academic Editor: János Nagy

Received: 09th May 2025

Revised: 13th June 2025

Accepted: 20th June 2025

Published: 15th July 2025

Copyright: © 2025 by the authors. Submitted for possible open access publication under the terms and conditions of the Creative Commons Attribution (CC BY) license (<https://creativecommons.org/licenses/by/4.0/>).

1. Introduction

Maize plays a key role in the global food supply and is also of major importance in animal feed and energy production [1,2]. It is the world's third most important cereal crop after wheat and rice and an essential ingredient in animal feed [3,4]. Its rapid growth [5] is contributing significantly to the continued expansion of the world's population and to maintaining food security in the face of climate change challenges [6,7]. The industrial use of maize is also expanding dynamically [8]. It has a wide range of uses, from sugar, oil, vinegar, beer, glucose, flour, dyes, soap, fuel and sustainable packaging [9-12]. In the last two decades, maize harvest has doubled [13]. The increase is mainly driven by the growing demand for animal feed and industrial use [14]. In Hungary, maize is the second largest crop after wheat, with an average annual area of 1 million hectares [15,16]. In 2023,

maize was harvested from 770.7 thousand hectares, with an average yield of 8.1 tonnes per hectare [17]. In maize (*Zea mays* L.) cultivation, accurate plant counting is essential for yield prediction and optimization of cultivation technology [18–20]. However, traditional manual counting methods such as manual plant counting have significant limitations including high error factors, time [21] while also damaging the plants [22] which may hinder their subsequent development. In recent years, the integration of geospatial technologies and advances in remote sensing have opened up new opportunities in agricultural data collection [23,24]. With the development of precision agriculture, the use of drones has become prominent in crop monitoring and plant counting [25]. The use of drones allows for fast and efficient data collection over large areas, minimizing the need for human resources and increasing accuracy. Aerial imagery with drones allows for rapid and detailed inspection of crop populations [26]. [27] has shown that accurate plant counts can be made using data collected by drones and advanced image processing algorithms, which helps to increase the accuracy of yield estimation [28,29]. Several researchers have investigated the relationship between plant number and NDVI. The NDVI value of a crop is related to yield [30–33], the strength of which depends largely on the stage of plant development at which the NDVI measurement was taken [30,34,35]. Research on maize has shown that NDVI values are strongly related to the number of plants and plant biomass. Some studies have shown that NDVI values measured during the growing season can be used to accurately estimate the number of plants and expected yield [36,37]. RGB images captured by UAV have been used [38] to successfully detect and count rice plants, [39] maize plants, [40] citrus trees and [41] grapevines. The use of drones in maize plant counts could revolutionize precision agriculture, enabling fast, accurate and cost-effective data collection [42,43]. Integrating technology into everyday farming practices will contribute to increased yields and more sustainable agricultural production. Our aim was to use a drone equipped with a multispectral camera to take stock images of maize after the phenological stage of emergence, and then use the images to count the number of emerged plants and determine its accuracy. This will give an idea of the success of the sowing, the heterogeneity of the stand and an estimate of the future yield.

2. Materials and Methods

2.1. Description of the experimental site

Our experiments were conducted in the 2007 sowing date duration experiment at the University of Debrecen, Institutes for Agricultural Research and Educational Farm (AKIT), Debrecen Landscape Farming and Landscape Research Institute (DTTI), Látókép Experimental Station (47° 83, 030" N, 21° 82, 060" E, 111 m a.s.l.) (Figure 1). The soil of the 2500 square metre, four replicate, random block design, small plot long-term experiment is a loess-formed, deep humic layer, medium plasticity, calcareous chernozem. The soil has a low tendency to acidification, as the 80–90 cm deep calcareous layer acts as an effective buffer against acidification. The physical composition is clay loam with a plasticity index of KA 42 according to Arany. The soil pH is 6.6. The humus content is medium (Hu%=2.6). The K₂O supply is good (240 mg kg⁻¹) and the P₂O₅ supply is medium (130 mg kg⁻¹) [44].

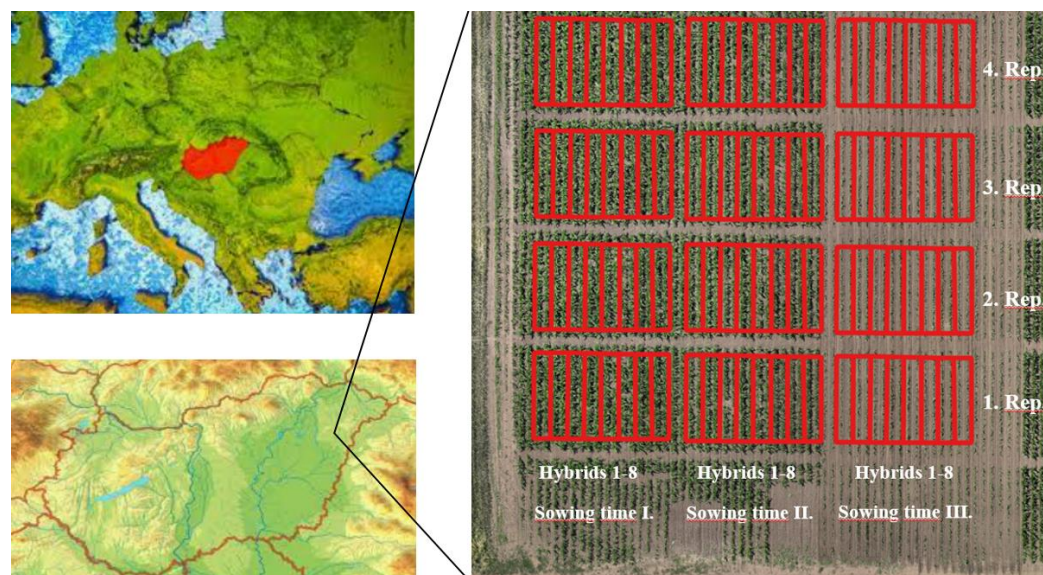


Figure 1. Arrangement of the sowing date experiment. Note: The sowing date experiment was founded in 2007 by Prof. Dr. Adrienn Kakuszi-Széles. Source: own construction

2.2. Layout and characteristics of the experimental space

The field experiment was carried out using three different sowing dates. In the 2024 growing season, Sowing Date I. was on 4 April, Sowing Date II. on 12 April and Sowing Date III on 3 May. Based on the soil samples taken prior to sowing, the initial water content was 16.67 m/m% at a depth of 0-20 cm, 18.01 m/m% at a depth of 20-60 cm and 18.32 m/m% at a depth of 60-100 cm. The same maize hybrids with 8-8 different genotypes were established at each sowing date. Each hybrid was sown in 2 rows, 4 replicates, at a rate of 72,200 plants per hectare. The sowing depth was 5 cm. Nutrient supplementation was achieved by basal fertilization in autumn (complex-10:26:26) followed by top dressing in spring ($\text{NH}_4\text{NO}_3 + \text{CaMg}(\text{CO}_3)_2$ - CAN). Herbicide Laudis was applied, and two mechanical treatments (cultivator) in the stand during the growing season helped the development of maize.

2.3. Weather characteristics

Weather data were collected using an automatic weather station 350 metres from the experiment. The weather during the maize growing season was generally unfavourable. At the beginning of the growing season, in April, a total of 38.3 mm of rain fell on 10 rainy days, 14.7 mm less than the long-term average (Figure 2). Rainfall in May (76.2 mm on 10 rainy days) was 12.2 mm above the 30-year average, which was favourable for maize. In terms of temperatures, a sharp cooling started on 14 April, with temperatures dropping more than 10°C in a few days. The monthly mean temperature was 13.6°C, 2.4°C above the multi-year average. Temperatures stabilised from the end of April, with a mean temperature of 17.5°C in May, 0.9°C above the 30-year average. Reference values are given for the period 1981-2010 (OMSZ 30-year average).

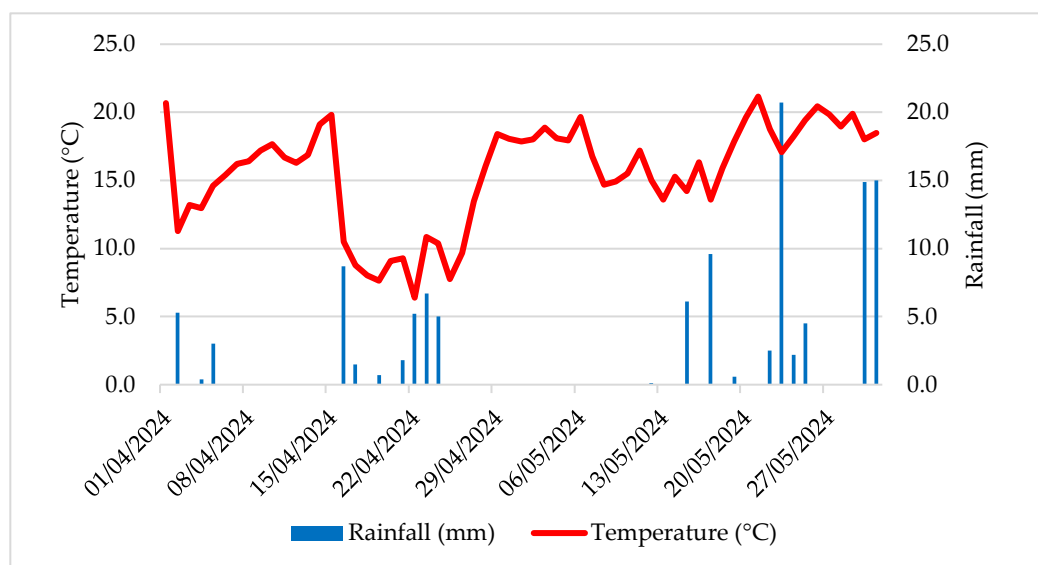


Figure 2. Weather patterns in the first third of the growing season (Debrecen-Látókép, 2024). Source: own construction

2.4. Statistical analysis

Statistical analysis was performed using Jamovi statistical software (version 2.3.28, open source software developed by the Jamovi Project) to measure the strength of the linear relationship using Pearson's correlation analysis.

2.5. Developing an accounting methodology

We were able to carry out the counts of maize using spectral data for the different sowing dates and the number of 2-4 leafed maize plants emerged for Sowing Date I and Sowing Date II. Taking into account all conditions (weather, field conditions), the population was recorded on 3 May 2024 using a DJI Mavic 3 drone equipped with a multispectral camera. The drone has 4 5 MP mono channel cameras and a 20 MP RGB camera. In addition, it is equipped with 8 safety cameras for obstacle avoidance. The near infrared (NIR: 860 nm \pm 26 nm) and red (Red - R: 650 nm \pm 26 nm) of the electromagnetic spectrum were used for the NDVI formula calculation. The flight parameters are shown in Table 1.

Table 1. Used flight parameters during the remote sensing (03.05.2024)

| | |
|------------------------------------|-------------------|
| Front and side overlap | 80 % |
| GSD (Ground Sampling Distance) | 1.84 cm/pixel |
| Altitude of the flight | 12 m AGL |
| Speed of the UAV during flight | 1 m/s |
| RTK base station distance | <20 km |
| Photo shooting | distance interval |
| Elevation optimization | turn ON |
| Angle of the camera | 90° |
| Reprojection error | <1 pixel |
| Angle of the flight | 150 ° |
| GCP (Ground Sampling Point) | not used |
| Light correction during the flight | automatically |

The first vegetation index is visible-light ($(NGRDI = \text{GREEN} - \text{RED}) / (\text{GREEN} + \text{RED})$), as the 20 megapixel RGB-based orthomosaics for the counting of the plots helped to improve the counting efficiency. The second vegetation index is a multispectral NDVI ($(NDVI = (\text{NIR} - \text{RED}) / (\text{NIR} + \text{RED}))$) vegetation index, was used for physiological comparisons of later phenological phases in V8-V10, VT, R6 phenological phases.

In our tests we used different GSD values, controlled by the WebODM software (version 2.6.0), open-source software developed by OpenDroneMap (ODM). When stitching the RGB images (Figure 3) (WebOdM software), we first performed the analyses with a resolution of 2.0 cm (A), and then with a resolution of 0.33 cm (B). The lower GSD value resulted in more accurate images with more information.

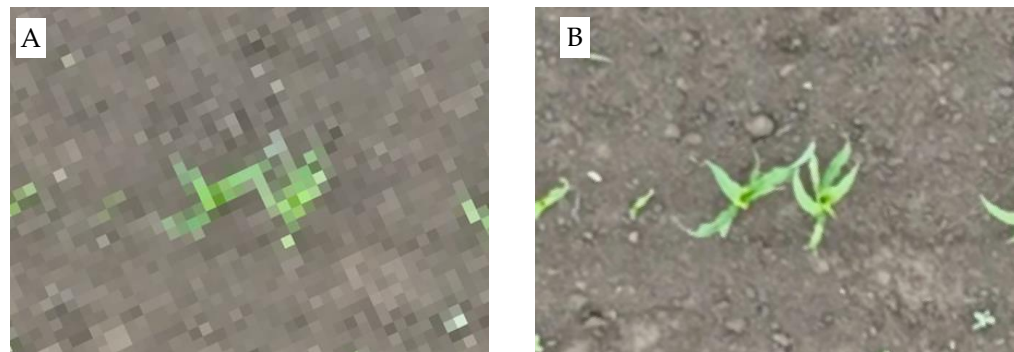


Figure 3 RGB images with different resolutions, (A) GSD=2 cm and (B) GSD= 0.3 cm

The geospatial analysis was carried out using the QGIS long term release software (version 3.36 "maidenhead", open-source software developed by the QGIS Project (QGIS.org)). NGRDI vegetation index was computed from the RGB image using raster calculator (Figure 4). The vegetation index layer was filtered to separate soil, shade and non-vegetation parts. The lower threshold for filtering was -0.072 and the upper threshold was 0.033.

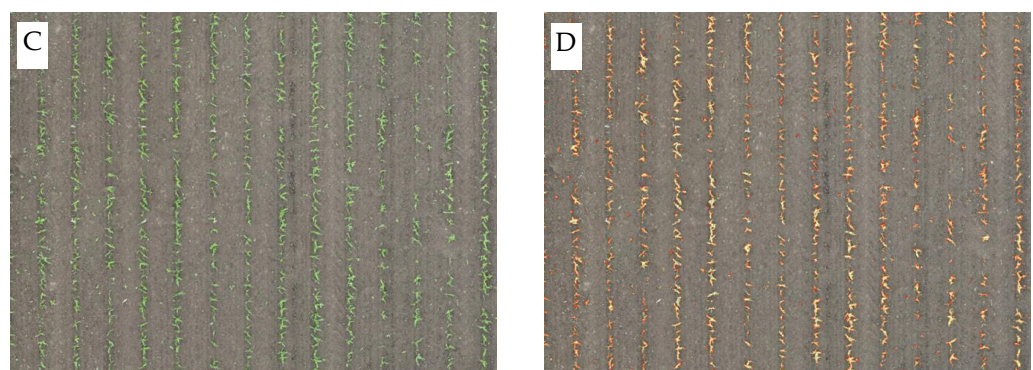


Figure 4: The (C) RGB orthomosaic and the (D) NGRDI orthomosaic calculated from the RGB image and after filtering.

The first orthomosaic (C) is a GSD=2 cm resolution image stitched from RGB images, from which a mask was created using NGRDI vegetation index. The second image shows the masked NGRDI image (D).

The RGB image was masked based on the NGRDI values and the cut mask was vectorized (Figure 5). The first image (E) shows the cut layer from the NGRDI image after masking, which was vectorized and sorted by size. Small pixels and pixel groups were

removed from the vectorized layer. The masked and vectorized image was filtered using a field calculator. During the filtering process, small plants and defects were removed from the image. The filtering was performed using a field calculator where the area of the individual vectors was determined using the following function and formula ($\$area * 10.000$). The area values of the "area" function were multiplied because the area function is normally defined in square meters and the function shows a value up to 3 decimal places, i.e. units with small areas were given a value of 0. Next, layer filtering was performed for pixel or pixel groups of less than 100 units area. Then, a polygon containing the parcels of the experimental area was extracted from the vector layer and points were placed in the center of the vectors using the centroids function (Figure 6, Figure 7). The points placed in the center of the vectors were counted using the number of pieces in the surface function, the result of which was integrated into the attribute table on a parcel by parcel basis. The analyses were carried out as follows with the same parameters for the area of the rows and then multiplied by two, so that the number of plants was counted with the polygon area of the plot smaller than the polygon area of the rows only, excluding any weeds in the row spacing.

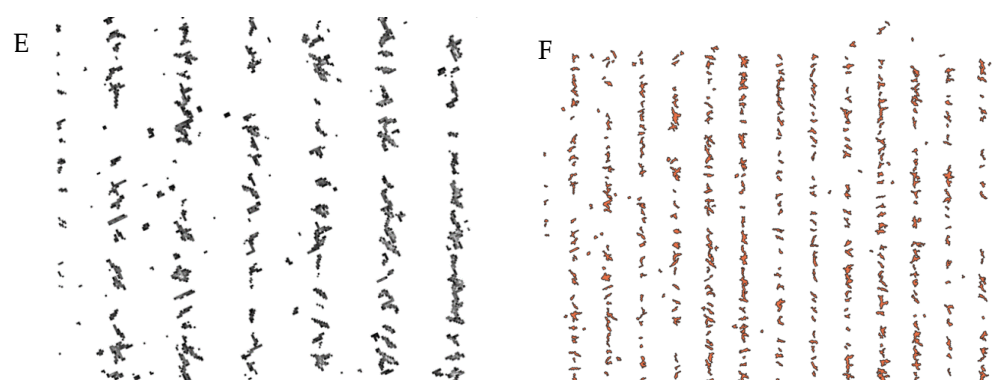


Figure 5. (E) Vectorise the raster layer and (F) filter the small vectors from the image to remove weeds and other distractions.

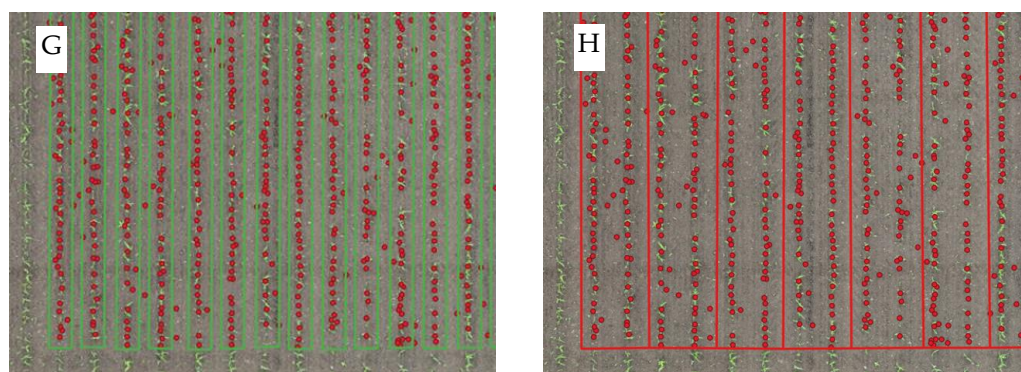


Figure 6. (E) Vectorise the raster layer and (F) filter the small vectors from the image to remove weeds and other distractions.

J

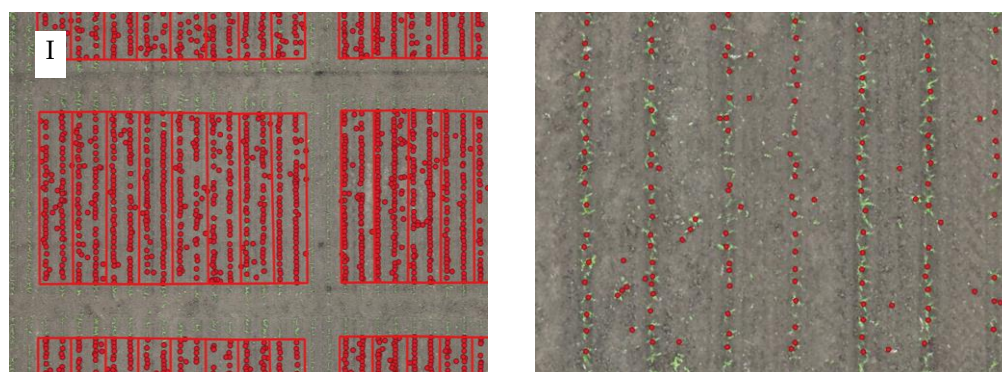


Figure 7. (I) Counting points on the surface using a function, (J) plants marks by points without polygon

To evaluate the results, we manually counted the number of plants in the images, which we took as the actual number of plants, and evaluated each of the plant number detection methodologies against this, and then validated the accuracy of the results as a function of plant number density using the NDVI vegetation index at three different dates, 6 June, 4 July and 23 August.

3. Results

Pearson's correlation analysis revealed a strong statistically valid correlation between the two measurement methods examined, number of plants/plot and number of plants/rowx2, with a r value of 0.977^{***} ($p < 0.001$) (Table 2). Among the NDVI values, the correlation between number of plants/rowx2 at the second measurement time was significant with $r = -0.418^{***}$. At the second time point, the NDVI value decreased as the density of plants per plot increased ($p < 0.001$). The results of the first recording time point 06.06 and the last recording time point 23.08 were not correlated with the density of plants per plot. For NDVI, the results of the negative NDVI values measured on 07.04 and 23.08.08 indicate that both recording methods show a decrease in the mean NDVI value without soil in the plot with increasing number of plants per plot. This result can be attributed to several ecological and plant life factors. Increasing the number of plants per hectare may increase competition between plants for light, water and nutrients, which may have a significant impact on photosynthetic activity and biomass development. With a high number of tillers, the foliage becomes denser, but light interception may be reduced as the lower leaves are shaded, which may reduce the amount of reflected near-infrared (NIR) radiation. In addition, plants may be subjected to increased stress, which may result in a decrease in chlorophyll content, further reducing NDVI values. If nutrient and water supplies are insufficient to sustain the increased plant population, the photosynthetically active area of vegetation may be reduced, resulting in lower NDVI values in overly dense stands.

Table 2 Pearson's correlation analysis between vegetation index values and counting methods.

| | | NDVI 06.06.2024 | NDVI 04.07.2024 | NDVI 23.08.2024 | Number of plants /plot |
|-----------------|-------------|--------------------|--------------------|--------------------|------------------------------|
| NDVI 04.07.2024 | Pearson's r | 0.420*** | - | | |
| | df | 62 | - | | |
| | p-value | < .001 | - | | |
| NDVI 23.08.2024 | Pearson's r | 0.175 | 0.386** | - | |
| | df | 62 | 62 | - | |
| | p-value | 0.166 | 0.002 | - | |

| | | | | | |
|------------------------|-------------|-------|-----------|--------|----------|
| number of plants/plot | Pearson's r | 0.035 | -0.415*** | -0.143 | - |
| | df | 62 | 62 | 62 | - |
| | p-value | 0.784 | < .001 | 0.261 | - |
| number of plants/rowx2 | Pearson's r | 0.037 | -0.418*** | -0,109 | 0.977*** |
| | df | 62 | 62 | 62 | 62 |
| | p-value | 0.773 | < .001 | 0.393 | < .001 |

Note: * p < 0.05, ** p < 0.01, *** p < 0.001

The relationship between the yield and the number of plants per plot. In examining the relationship between yield and number of plants per plot, we found that, on average, yield was not associated with any of the hybrid measurements, with r values of 0.109 and 0.163 (p=0.390, p=0.198) (Table 3). These results suggest that the hybrids compensated well for differences in yield due to seeding or emergence and that this did not translate into increases or decreases in yield.

Table 3 Pearson's correlation analysis between the yield and counting methods.

| | | Number of plants /plot | Number of plants / rowx2 | Yield (t ha ⁻¹) |
|-----------------------------|-------------|------------------------|--------------------------|-----------------------------|
| yield (t ha ⁻¹) | Pearson's r | 0.109 | 0.163 | - |
| | df | 62 | 62 | - |
| | p-value | 0.390 | 0.198 | - |

Note: * p < 0.05, ** p < 0.01, *** p < 0.001

In our tests, we compared the measurement methods with the actual number of plants counted manually in the plots (Table 4). Our results show that the degree of correlation between the actual and the developed measurement methods for determining the number of head increased as the different settings were refined.

Table 4 Pearson's correlation analysis between the measured and the real number of plants

| | | Number of plants /plot (GSD 2 cm) | Number of plants / rowx2 (2 cm) | Number of plants /plot (GSD 0.33) | Number of plants / rowx24 (GSD 0.33) |
|-------------------------------------|-------------|-----------------------------------|---------------------------------|-----------------------------------|--------------------------------------|
| number of plants/rowx2 (2 cm) | Pearson's r | 0.977*** | - | | |
| | p-value | < .001 | - | | |
| number of plants /plot (GSD 0,33) | | 0.921*** | 0.900*** | - | |
| | | < .001 | < .001 | - | |
| number of plants / rowx2 (GSD 0,33) | Pearson's r | 0.895*** | 0.918*** | 0.969*** | - |
| | p-value | < .001 | < .001 | < .001 | - |
| real number of plants/plots | Pearson's r | 0.659*** | 0.691*** | 0.700*** | 0.737*** |
| | p-value | < .001 | < .001 | < .001 | < .001 |

Note: * p < 0.05, ** p < 0.01, *** p < 0.001

An r value of 0.659*** was measured between the real number of plants/plot and the number of plants/plot (GSD 2 cm) ($p < 0.001$). The strength of this relationship increased steadily when the row widths of the plots were filtered and the number of plants/rowx2 (2 cm) method was applied, where r value is 0.691*** ($p < 0.001$). Thus, if we use a GSD of 2 cm and filter out the confounding factors in the row spacing and measure only the rows, the drone count becomes more accurate. After refining the measurements, the images were analysed at GSD values of 0.33 cm, where the correlation between the real number of plants/plot and the number of plants/plot (GSD 0.33) was 0.700*** ($p < 0.001$). Similarly, rowx2 was filtered out in the higher resolution image, where this resulted in an increase in the size of the correlation between the real number of plants/plot and a number of plants/rowx2 (GSD 0.33) $r=0.737$ *** ($p < 0.001$).

4. Discussion

Similar to the results of [45] and [46], post-emergence maize counts using drones equipped with multispectral cameras allow precise, rapid and large-area data collection. This form of remote sensing can minimize errors due to manual sampling and can significantly reduce time and labor requirements, as well as provide the opportunity for inventory collection in poorer environmental conditions.

There is a strong significant correlation between the two measurement methods presented in this paper, number of plants/plot and number of plants/rowx2, with an r value of 0.977*** ($p < 0.001$). A correlation between the number of plants counted and NDVI values was observed, in line with the findings of [47]. At the second measurement date (4 July), the correlation between number of plants/rowx2 was significant with $r=-0.418$ ***. Similar to the results of [48], the measurement and evaluation of NDVI proved to be effective in identifying the number of plants. As the number of plants per plot increased, the mean NDVI value without soil in the plot decreased, suggesting that competition between plants due to increasing number of plants may affect photosynthetic activity and biomass development, similar to the findings of [49]. Shading of the lower leaves may reduce the amount of reflected NIR radiation, and reduced chlorophyll quantity due to stress may also reduce the NDVI value.

Similarly, to the results of [50] and [51], the correlation analysis between number of plants and yield showed that the hybrids included in the study compensated well for differences in number of plants due to sowing or emergence and this did not translate into an increase or decrease in yield ($r=0.109$ and 0.163 ($p=0.390$ and 0.198)). Thus, it can be concluded that maize responds flexibly to changes in number of plants without significant yield loss.

5. Conclusions

Our results show that the correlation between the actual and the developed measurement methods for the determination of the number of plants has increased as the different settings have been refined.

By using the census method and results to identify germination imbalances, farmers can make timely corrections to their crop management strategies, such as targeted replenishment, nutrient replenishment or crop protection interventions. Knowing the exact number of plants can also be important for subsequent agrotechnical decisions. Ensuring the right number of plants can improve the conditions of competition between crops, increasing the yield average. Our results pertain to a single growing season, and based on

these values, it is not possible to determine a long-term trend or a relationship between plant density and yield. This study merely provides a direction and raises further research questions. Differential application of nutrient supply and crop protection can make production more cost-effective. Knowing the number of plants and their developmental status can help to make more accurate yield forecasts, which can help with logistical and marketing decisions. Poorly germinated stands can indicate soil defects, sowing problems or the presence of pathogens which can be addressed by early intervention.

Author Contributions: A.S., P.Z. and É.H. carried out the experimental design. P.Z., Á.I. and É.H. performed the experiments. A.S. and Á.I. made the statistical analysis. C.B., Á.I., P.Z., É.H. and A.S. prepared the manuscript and coordinated its revision. C.B., A.S., É.H. read and revised the manuscript. All authors have read and agreed to the published version of the manuscript.

Funding: Project no. TKP2021-NKTA-32 has been implemented with the support provided by the Ministry of Culture and Innovation of Hungary from the National Research, Development and Innovation Fund, financed under the TKP2021-NKTA funding scheme and supported by the EKÖP-24-4 University Research Scholarship Program of the Ministry for Culture and Innovation from the source of the National Research, Development and Innovation Fund. This paper was also supported by the János Bolyai Research Scholarship of the Hungarian Academy of Sciences (BO/00068/23/4).

Data Availability Statement: All the data supporting the conclusions of this article are included in this article.

Conflicts of Interest: The authors declare no conflict of interest.

References

- Hou, P.; Liu, Y.; Liu, W.; Liu, G.; Xie, R.; Wang, K.; Ming, B.; Wang, Y.; Zhao, R.; Zhang, W.; Wang, Y.; Bian, S.; Ren, H.; Zhao, X.; Liu, P.; Chang, J.; Zhang, G.; Liu, J.; Yuan, L.; Zhao, H.; Shi, L.; Zhang, L.; Yu, L.; Gao, J. L.; Yu, X.; Shen, L.; Yang, S.; Zhang, Z.; Xue, J.; Ma, X.; Wang, X.; Lu, T.; Dong, B.; Li, G.; Ma, B.; Li, J.; Deng, X.; Liu, Y.; Yang, Q.; Fu, H.; Liu, X.; Chen, X.; Huang, C.; Li, S. How to increase maize production without extra nitrogen input. *Resour. Conserv. Recycl.* **2020**, *160*, 104913, 1–9.
- Széles, A.; Horváth, É.; Simon, K.; Zagyai, P.; Huzsvai, L. Maize Production under Drought Stress: Nutrient Supply, Yield Prediction. *Plants-Basel*. **2023**, *12*, 18, 3301, 1–17. <https://doi.org/10.3390/plants12183301>
- Shiferaw, B.; Prasanna, B. M.; Hellin, J.; Bänziger, M. Crops that feed the world 6. Past successes and future challenges to the role played by maize in global food security. *Food Secur.* **2011**, *3*, 307–327.
- Malaviarachchi, M.A.P.W.K.; De Costa, W.A.J.M.; Fonseka, R.M.; Kamara, J.B.D.A.P.; Abhayapala, K.M.R.D.; Suriyagoda, L.D.B. Response of maize (*Zea mays* L.) to a temperature gradient representing long-term climate change under different soil management systems. *Tropical Agriculture Research*. **2015**, *25*, 3, 327–344.
- Nagy, J. *Maize production: Food, bioenergy, forage*. Akadémiai kiadó, Budapest, 2008; 391 p.
- Nagy, J. *Kukorica*. Szaktudás Kiadó, Budapest, 2021; 516 p.
- Khatibi, A.; Omrani, S.; Omrani, A.; Shojaei, S.H.; Mousavi, S.M.N.; Illés, Á.; Bojtor, C.; Nagy, J. Response of maize hybrids in drought-stress using drought tolerance indices. *Water*. **2022**, *14*, 7, 1012, 1–10. <https://doi.org/10.3390/w14071012>
- Listman, M.; Ordóñez, R. Ten things you should know about maize and wheat. International Maize and Wheat Improvement Center (CIMMYT). www.cimmyt.org/news/ten-things-you-should-know-about-maize-and-wheat/. **2019**.
- Harsányi, E.; Rátónyi, T.; Kiss, Cs.; Juhász, Cs. How does maize-based bioethanol production contribute to energy production and employment in Hungary. In: *13th Ramiran International Conference Potential for simple technology solutions in organic manure management*, Koutev, V. (ed.); pp. 323–326.
- Uarrota, V.G.; Schmidt, E.C.; Bouzon, Z.L.; Maraschin, M. Histochemical Analysis and Protein Content of Maize Landraces (*Zea mays* L.). *J. Agron.* **2011**, *10*, 92–98.
- Karn, A.; Gillman, J.D.; Flint-Garcia, S.A. Genetic analysis of teosinte alleles for kernel composition traits in maize. *G3: Genes, Genomes, Genetics*. **2017**, *7*, 1157–1164.
- Rátónyi, T.; Ragán, P.; Nagy, J.; Harsányi, E. A kukorica alapú bioetanol előállítás eredményességének vizsgálata. In *Hangsúlyok a térfejlesztésben* Nagy J. (ed.); DE MÉK, Debrecen, 2018; pp. 355–369.

13. FAO. „Crops and livestock products”. <https://www.fao.org/faostat/en/#data/QCL/visualize>. 2024.
14. Oláh, J.; Popp, J. A kukoricatermelés kilátásai. *Magyar Mezőgazdaság*. **2018**.
15. Nagy, J. Magyarország földhasználatának 150 éve (1868-2018). *Növénytermelés*. **2018**, *67*, 3, 51–72.
16. Ssemugenze, B.; Ocwa, A.; Bojtor, C.; Illés, Á.; Esimu, J.; Nagy, J. Impact of research on maize production challenges in Hungary. *Heliyon*. **2024**, *10*, 6, e26099, <https://doi.org/10.1016/j.heliyon.2024.e26099>
17. KSH. A kukorica termelése vármegye és régió szerint. https://www.ksh.hu/stadat_files/mez/hu/mez0072.html. 2024.
18. Pu, H.; Chen, X.; Yang, Y.; Tang, R.; Luo, J.; Wang, Y.; Mu, J. Tassel-YOLO: A new high-precision and real-time method for maize tassel detection and counting based on UAV aerial images. *Drones*. **2023**, *7*, 8, 492.
19. Chen, J.; Fu, Y.; Guo, Y.; Xu, Y.; Zhang, X.; Hao, F. An improved deep learning approach for detection of maize tassels using UAV-based RGB images. *Int. J. Appl. Earth Obs. Geoinf.* **2024**, *130*, 103922.
20. Song, C.; Zhang, F.; Xie, J.; Yang, C.; Li, J.; Zhang, J. Development and evaluation of a novel maize detasseling device. *Computers and Electronics in Agriculture*. **2024**, *221*, 108944.
21. Guo, Y.; Fu, Y.H.; Chen, S.; Bryant, C.R.; Li, X.; Senthilnath, J.; Sun, H.; Wang, S.; Wu, Z.; de Beurs, K. Integrating spectral and textural information for identifying the tasseling date of summer maize using UAV based RGB images. *Int. J. Appl. Earth Obs. Geoinf.* **2021**, *102*, 102435.
22. Kumar, A.; Desai, S.V.; Balasubramanian, V.N.; Rajalakshmi, P.; Guo, W.; Naik, B.B.; Balram, M.; Desai. Efficient maize tassel-detection method using UAV based remote sensing. *Remote Sensing Applications: Society and Environment*. **2021**, *23*, 100549.
23. Huang, Y.; Chen, Z.X.; Tao, Y.U.; Huang, X.Z.; Gu, X.F. Agricultural remote sensing big data: Management and applications. *J. Integr. Agric.* **2018**, *17*, 9, 1915–1931.
24. Omia, E.; Bae, H.; Park, E.; Kim, M. S.; Baek, I.; Kabenge, I.; Cho, B. K. Remote sensing in field crop monitoring: A comprehensive review of sensor systems, data analyses and recent advances. *Remote Sens.* **2023**, *15*, 2, 354.
25. Yang, H.; Wu, J.; Lu, Y.; Huang, Y.; Yang, P.; Qian, Y. Lightweight Detection and Counting of Maize Tassels in UAV RGB Images. *Remote Sens.* **2024**, *17*, 1, 3.
26. Olson, D.; Anderson, J. Review on unmanned aerial vehicles, remote sensors, imagery processing, and their applications in agriculture. *Agronomy Journal*. **2021**, *113*, 2, 971–992.
27. Könczöl, P. A tőszám- és terméskomponens-vizsgálatok eredményeinek felhasználása a kukorica gyakorlati nemesítői munkában. In *XXIII. Növénytermesztési Tudományos Nap: Összefoglalók*. Ed.: Veisz Ottó, Magyar Tudományos Akadémia, Budapest, 2017, 53.
28. Guebsi, R.; Mami, S.; Chokmani, K. Drones in precision agriculture: A comprehensive review of applications, technologies, and challenges. *Drones*, **2024**, *8*, 11, 686.
29. Fan, J.; Zhou, J.; Wang, B.; de Leon, N.; Kaeppler, S. M.; Lima, D. C.; Zhang, Z. Estimation of maize yield and flowering time using multi-temporal UAV-based hyperspectral data. *Remote Sens.* **2022**, *14*, 13, 3052.
30. Teal, R.K.; Tubana, B.; Girma, K.; Freeman, K.W.; Arnall, D. B.; Walsh, O.; Raun, W.R. In-season prediction of corn grain yield potential using Normalized Difference Vegetation Index. *Agronomy Journal*. **2006**, *98*, 6, 1488–1494.
31. Cui, D.; Li, M.; Zhang, Q. Development of an optical sensor for crop leaf chlorophyll content detection. *Computers and Electronics in Agriculture*. **2009**, *69*, 2, 171–176.
32. Tamás, A.; Kovács, E.; Horváth, É.; Juhász, C.; Radócz, L.; Rátonyi, T.; Ragán, P. Assessment of NDVI dynamics of maize (*Zea mays* L.) and its relation to grain yield in a polyfactorial experiment based on remote sensing. *Agriculture*. **2023**, *13*, 3, 689.
33. Kumar, D. A.; Neelima, T. L.; Srikanth, P.; Devi, M. U.; Suresh, K.; Murthy, C. S. Maize yield prediction using NDVI derived from Sentinel 2 data in Siddipet district of Telangana state. *J. Agrometeorol.*, **2022**, *24*, 2, 165–168.
34. Aparicio, N.; Villegas, D.; Casadesus, J.; Araus, J.L.; Royo, C. Spectral vegetation indices as nondestructive tools for determining durum wheat yield. *Agronomy Journal*. **2000**, *92*, 1, 83–91.
35. Chung, B.; Girma, K.; Martin, K.L.; Tubaña, B.S.; Arnall, D.B.; Walsh, O.; Raun, W.R. Determination of optimum resolution for predicting corn grain yield using sensor measurements. *Arch. Agron. Soil Sci.* **2008**, *54*, 5, 481–491.
36. Wahab, I.; Hall, O.; Jirstrom, M. Remote sensing of yields: Application of uav imagery-derived ndvi for estimating maize vigor and yields in complex farming systems in sub-saharan africa. *Drones*. **2018**, *2*, 3, 28.
37. Maresma, A.; Chamberlain, L.; Tagarakis, A.; Kharel, T.; Godwin, G.; Czymmek, K.J.; Shields, E.; Ketterings, Q.M. Accuracy of NDVI-derived corn yield predictions is impacted by time of sensing. *Computers and electronics in agriculture*. **2020**, *169*, 105236.

38. Bai, X.; Liu, P.; Cao, Z.; Lu, H.; Xiong, H.; Yang, A.; Cai, Z.; Wang, J.; Yao, J. Rice plant counting, locating, and sizing method based on high-throughput UAV RGB images. *Plant Phenomics*. **2023**, *5*, 0020.
39. Yadav, P.K.; Thomasson, J.A.; Hardin, R.; Searcy, S.W.; Braga-Neto, U.; Popescu, S.C.; Martin, D.E.; Rodriguez, R.; Meza, K.; Enciso, J.; Diaz, J.S.; Wang, T. Detecting volunteer cotton plants in a corn field with deep learning on UAV remote-sensing imagery. *Computers and Electronics in Agriculture*. **2023**, *204*, 107551.
40. Zheng, Z.; Wu, M.; Chen, L.; Wang, C.; Xiong, J.; Wei, L.; Huang, X.; Wang, S.; Huang, W.; Du, D. A robust and efficient citrus counting approach for large-scale unstructured orchards. *Agricultural Systems*. **2024**, *215*, 103867.
41. Ariza-Sentís, M.; Baja, H.; Vélez, S.; Valente, J. Object detection and tracking on UAV RGB videos for early extraction of grape phenotypic traits. *Computers and Electronics in Agriculture*. **2023**, *211*, 108051.
42. Velusamy, P.; Rajendran, S.; Mahendran, R. K.; Naseer, S.; Shafiq, M.; Choi, J. G. Unmanned Aerial Vehicles (UAV) in precision agriculture: Applications and challenges. *Energies*. **2021**, *15*, 1, 217.
43. Zuolkernan, I.; Abuhani, D. A.; Hussain, M. H.; Khan, J.; ElMohandes, M. Machine learning for precision agriculture using imagery from unmanned aerial vehicles (uavs): A survey. *Drones*. **2023**, *7*, 6, 382.
44. Széles, A.; Horváth, É.; Huzsvai, L. A vetésidő, az időjárás és a kukoricaszem fehérje- és olajtartalma közötti kapcsolat eltérő genotípusú kukorica hibrideknél. *Növénytermelés*. **2020**, *69*, 3, 115–135.
45. Varela, S.; Dhodda, P.R.; Hsu, W.H.; Prasad, P.V.; Assefa, Y.; Peralta, N.R.; Griffin, T.; Aharda, A.; Ferguson, A.; Ciampitti, I.A. Early-season stand count determination in corn via integration of imagery from unmanned aerial systems (UAS) and supervised learning techniques. *Remote Sensing*. **2018**, *10*, 2, 343.
46. Vong, C. N. Quantifying Corn Emergence Using UAV Imagery and Machine Learning (Doctoral dissertation, University of Missouri-Columbia). **2022**.
47. Alharbi, S.; Raun, W.R.; Arnall, D.B.; Zhang, H. Prediction of maize (*Zea mays* L.) population using normalized-difference vegetative index (NDVI) and coefficient of variation (CV). *J. Plant Nutr.* **2019**, *42*, 6, 673–679.
48. Vian, A. L.; Bredemeier, C.; Drum, M.A.; Pires, J.L.F.; Fochesatto, E. Vegetation sensors as a tool for plant population identification and corn grain yield estimation. *Pesqui. Agropecu. Trop.* **2021**, *51*, e66926.
49. Salifu, M.; Dóka, L.F. Effects of plant density on photosynthetic characteristics and yield of maize under irrigation condition. *Acta Agraria Debreceniensis*. **2019**, *1*, 115–118.
50. Lacasa, J.; Gaspar, A.; Hinds, M.; Jayasinghege Don, S.; Berning, D.; Ciampitti, I.A. Bayesian approach for maize yield response to plant density from both agronomic and economic viewpoints in North America. *Sci. rep.* **2020**, *10*, 1, 15948.
51. Dong, Y.; Feng, Z.; Li, T.; Farhan, A.; Tian, X.; Lao, Y.; Duan, Y.; Si, L.; Zhang, X.; Xue, J.; Xu, S. Performance and stability of yield in response to plant density, year and location in maize hybrids of Northwest China. *Technol. Agron.* **2022**, *2*, 1, 1–7.

Disclaimer/Publisher’s Note: All views, interpretations, and data presented in these publications are exclusively those of the respective authors and contributors, and do not represent the positions of PCP or its editors. PCP and its editorial team assume no liability for harm or damage to persons or property that may arise from the use of concepts, techniques, guidance, or products discussed within the published material.